Supplemental Material

Charge density wave instability and pressure-induced superconductivity in bulk 1T-NbS$_2$

Wei Wang,[1] Bosen Wang,[2] Zhibin Gao,[3] Gang Tang,[4] Wen Lei, [1] Xiaojun Zheng,[1] Huan Li,[1] Xing Ming,[1*] and Carmine Autieri[5†]

1. College of Science, Guilin University of Technology, Guilin 541004, China

2. Beijing National Laboratory for Condensed Matter Physics and Institute of Physics, Chinese Academy of Sciences, Beijing 100190, China

3. Department of Physics, National University of Singapore, Singapore 117551, Republic of Singapore

4. Theoretical Materials Physics, Q-MAT, CESAM, University of Liège, B-4000 Liège, Belgium

5. International Research Centre MagTop, Institute of Physics, Polish Academy of Sciences, Aleja Lotników 32/46, PL-02668 Warsaw, Poland

[*] Email: mingxing@glut.edu.cn (Xing Ming)
[†] Email: autieri@magtop.ifpan.edu.pl (Carmine Autieri)

Table S1 Atomic Wyckoff positions of the CCDW phase

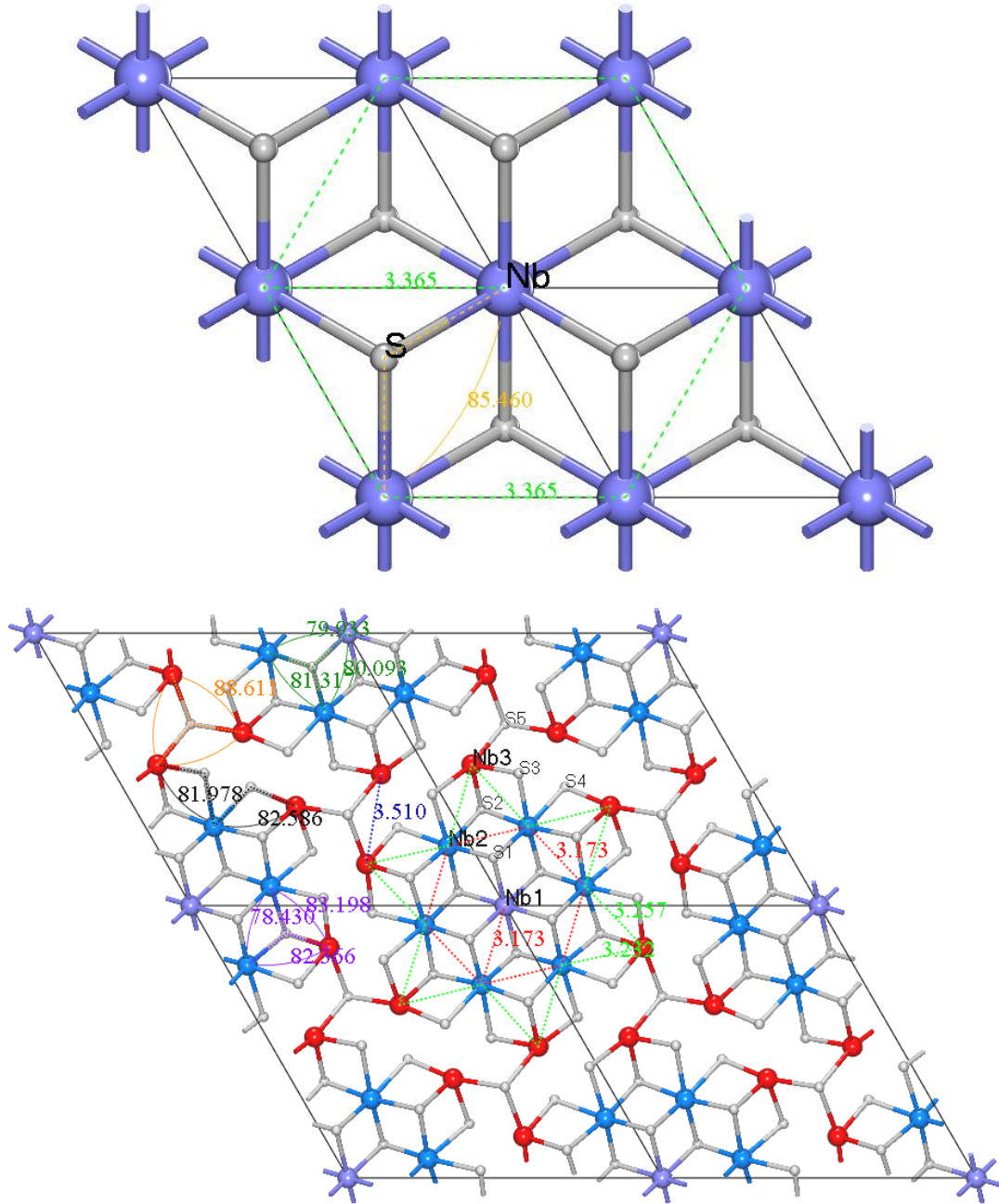| Atom	Wyckoff site	x	y	z
Nb	1a	0.00000	0.00000	0.00000
Nb	6g	0.28895	0.07091	0.00079
Nb	6g	0.63544	0.15267	0.99709
S	6g	0.05081	0.17504	0.27403
S	6g	0.35420	0.25173	0.27096
S	6g	0.48565	0.19924	0.75082
S	6g	0.97298	0.40846	0.24565
S	2d	0.33333	0.66667	0.75405

Fig. S1 Vertical view of the optimized crystal structure for the undistorted high-symmetry phase (top) and distorted CCDW phase (bottom) of bulk $1T$-NbS$_2$. Compared to the undistorted phase, there are three nonequivalent Nb atoms sites in the CCDW phase: The central Nb atoms in the star (purple), the peripheral Nb atoms belonging to the $\sqrt{7} \times \sqrt{7}$ cluster (blue), and more peripheral Nb atoms sites (red). These three kinds of Nb atoms form $\sqrt{13} \times \sqrt{13}$ star-of-David clusters schematized by green lines. The S atoms are shown in gray balls. The Nb-Nb distances and Nb-S-Nb bond angles are shown by the numbers.
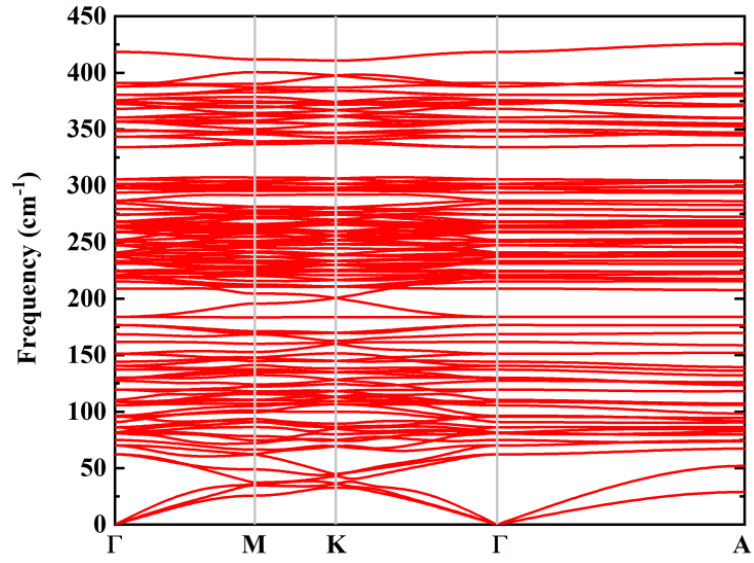
Fig. S2 Phonon dispersion curves for the $\sqrt{13} \times \sqrt{13}$ CCDW phase of bulk $1T$-NbS$_2$ calculated by VASP joint with Phonopy code within 1×1×2 supercell (78 atoms).
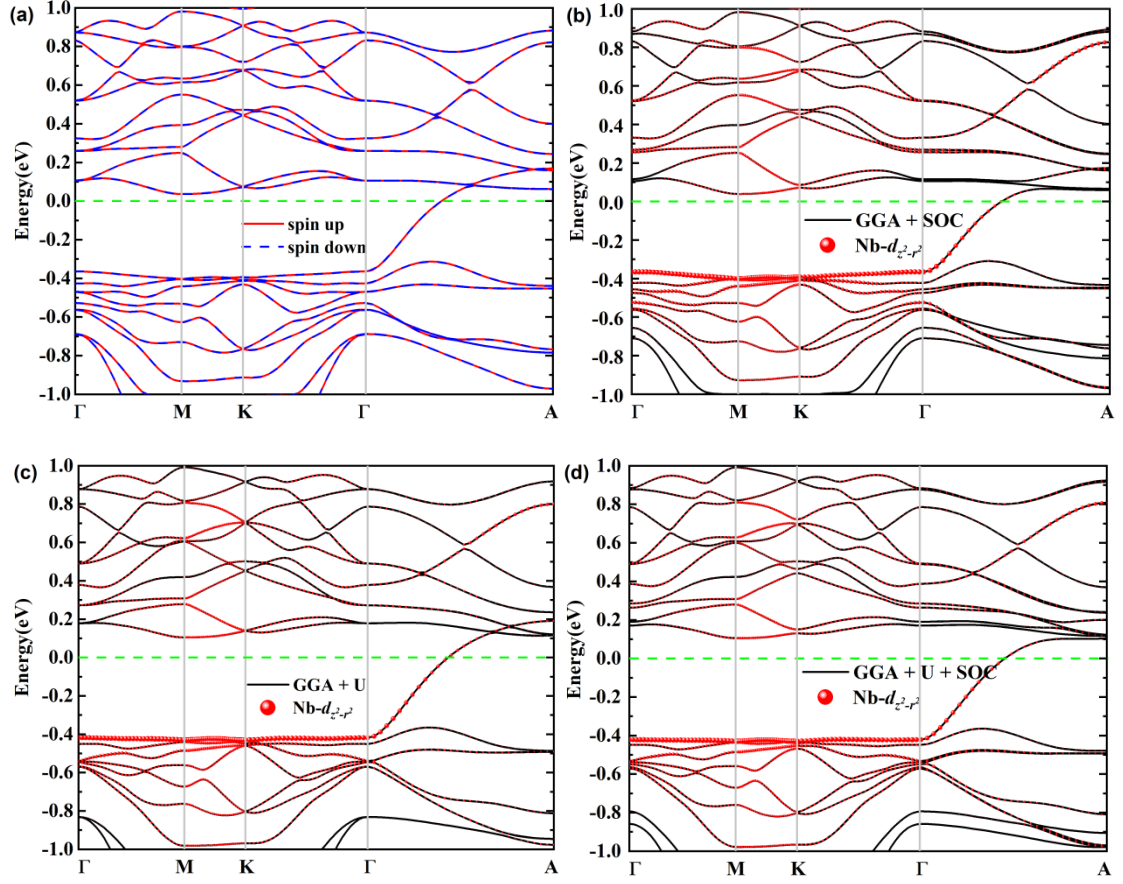
Fig. S3 Electronic band structures of the $\sqrt{13} \times \sqrt{13}$ CCDW phase within 1×1×1 cell calculated with (a) spin polarized GGA, (b) GGA+SOC (c) GGA + U, and (d) GGA + U + SOC. The red balls represent orbital contributions with the $d_{z^2-r^2}$ character. We use U value of 2.95 eV here.
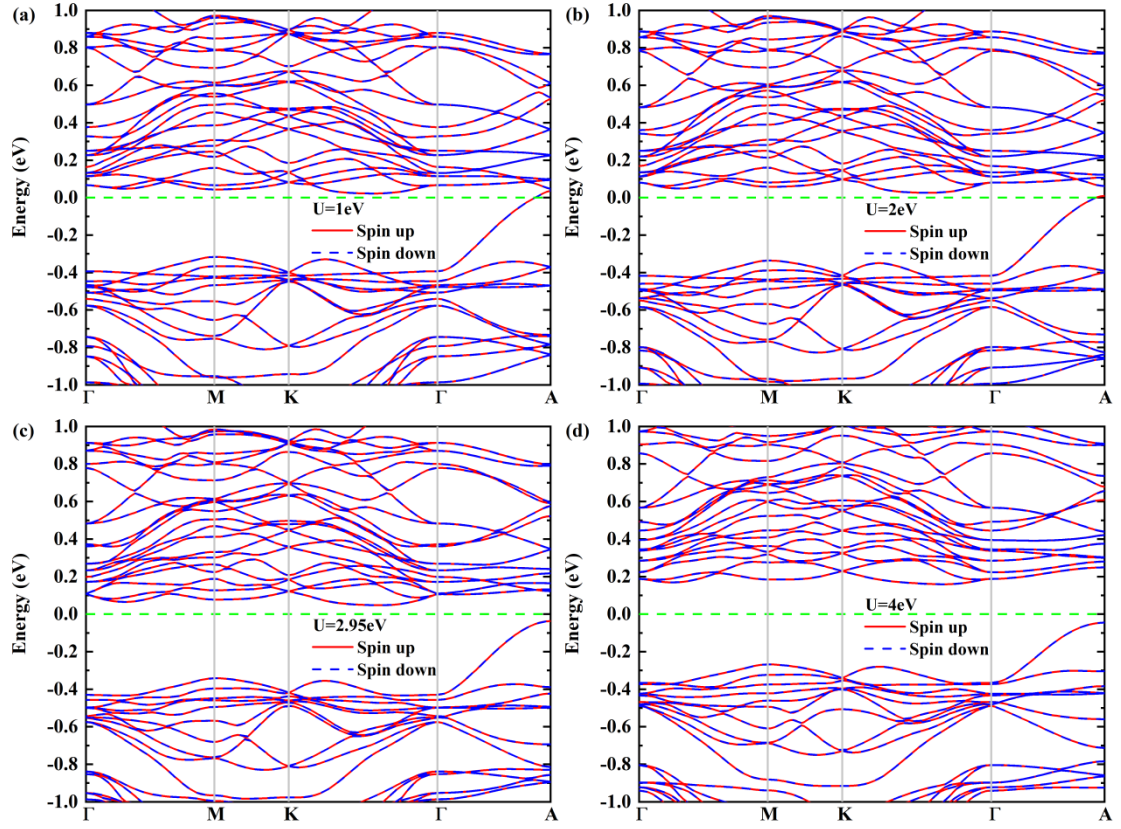
Fig. S4 Antiferromagnetic electronic band structure of the $\sqrt{13} \times \sqrt{13}$ CCDW phase within $1\times1\times2$ supercell calculated by GGA + U with different U values.
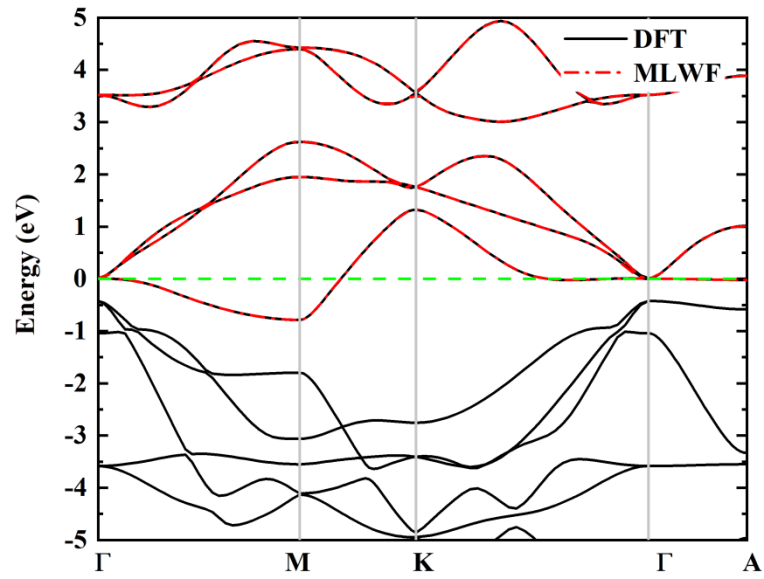
Fig. S5 Band structure of the bulk 1T-NbS$_2$ in the high-symmetry phase calculated by first principles based on DFT (black solid lines) and 5-orbital d band model within the MLWF method (red dashed lines).
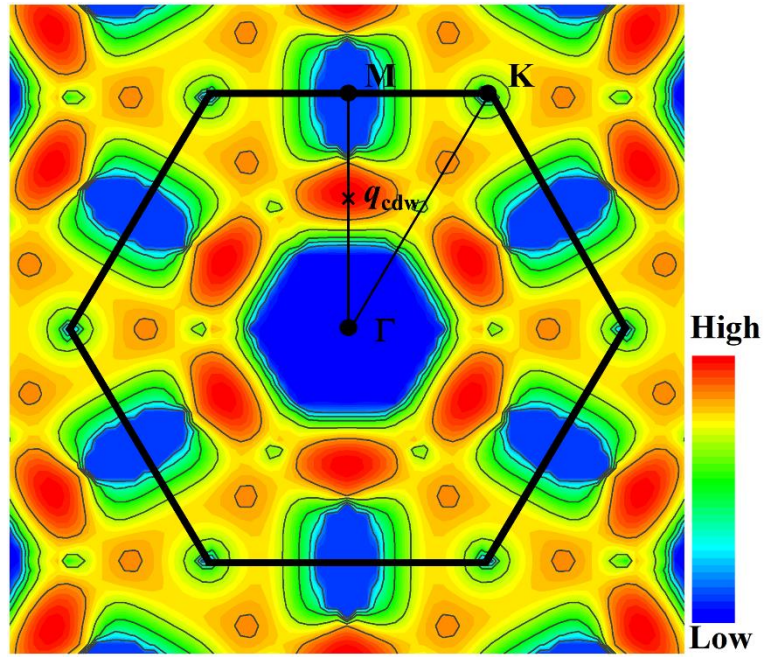
Fig. S6 Phonon linewidth of the lowest phonon mode in the $q_z = 0$ plane, which is calculated within a normal smearing parameter σ of 0.01 Ry for the undistorted high-symmetry $1T$-NbS$_2$. The corresponding phonon dispersion curves have been presented in Fig. 2(c) of the main text. The color bar indicates the relative value.
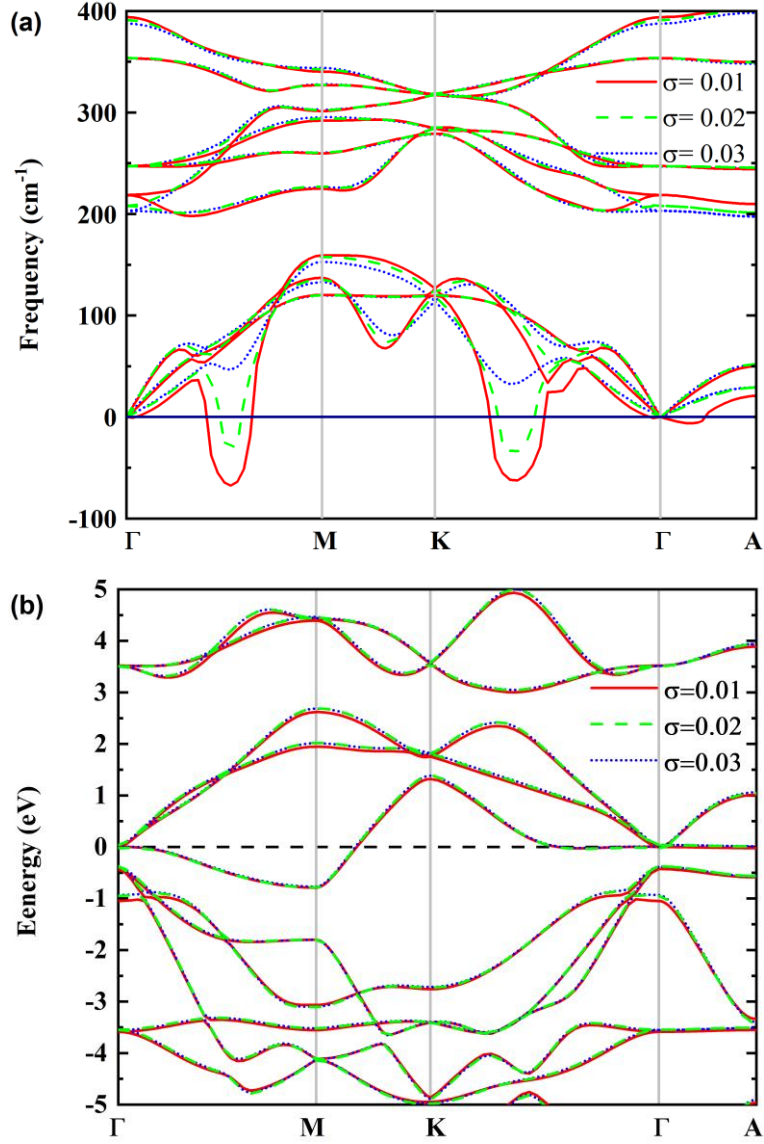
Fig. S7 (a) Phonon dispersion curves and (b) electronic band structure of the undistorted high symmetry 1T-NbS$_2$ calculated within different smearing parameter σ by *QUANTUM ESPRESSO* package. The band structures are calculated with almost identical relaxed lattice constants by smearing parameter σ= 0.01, 0.02, and 0.03 Ry, where a = 3.365, 3.351 and 3.356 Å, and c = 5.954, 5.889 and 5.883 Å, respectively. Larger σ indeed removes the imaginary phonon mode, whereas the smearing parameter almost plays no role in the lattice constants and band structures.
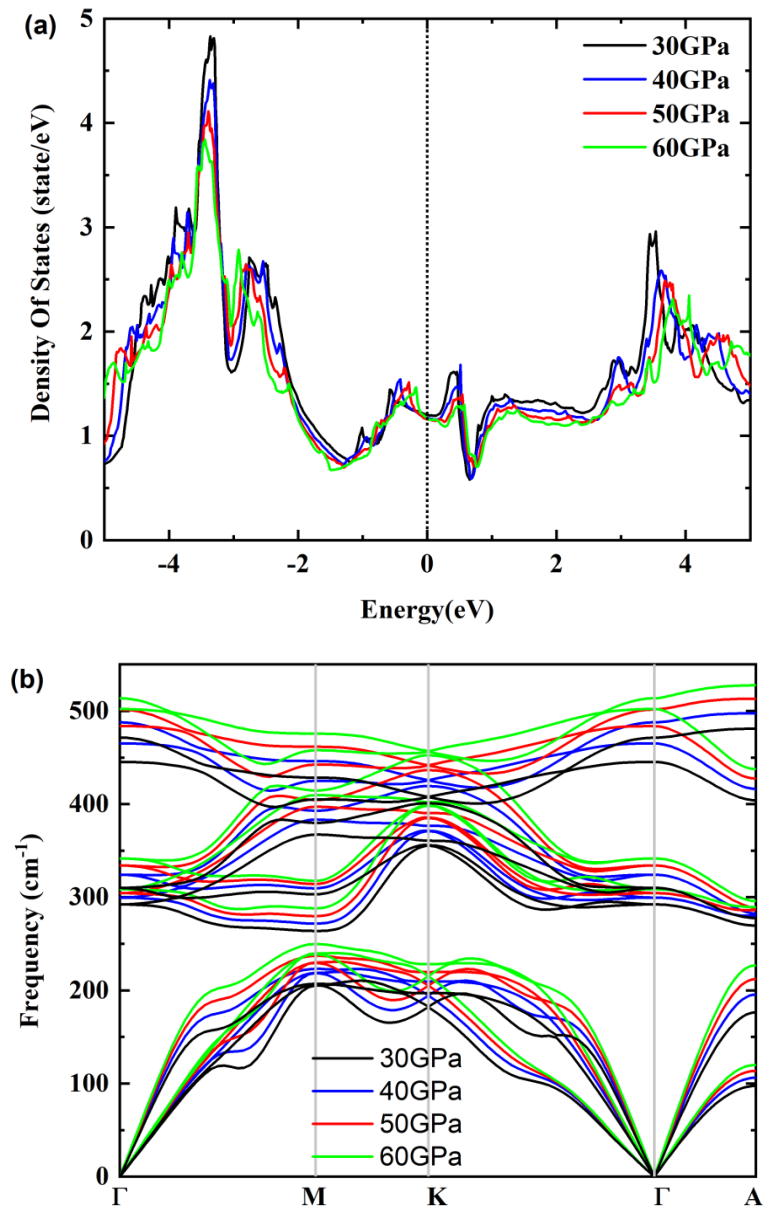
Fig. S8 (a) Electronic density of states and (b) phonon dispersion curves for the superconducting phase of the compressed bulk 1*T*-NbS$_2$ at different pressure.